Carbon Nanotube, Carbon Black and Copper Nanoparticle Modified Screen Printed Electrodes for Amino Acid Determination

Ricardo C. Carvalho,[a] *Adil Mandil*,[b] *Krishna P. Prathish*,[a] *Aziz Amine*,[b] *Christopher M. A. Brett**[a]

[a] Departamento de Química, Faculdade de Ciências e Tecnologia, Universidade de Coimbra, 3004-535 Coimbra, Portugal
tel: +351-239854470; fax: +351-239827703
[b] Laboratory of Chemical Analysis and Biosensors, Faculty of Sciences and Techniques, University Hassan II Mohammedia, 20850-Mohammedia, Morocco
*e-mail: brett@ci.uc.pt

Received: September 13, 2012
Accepted: October 15, 2012
Published online: December 7, 2012

Abstract
Screen-printed electrodes have been used for the determination of amino acids, focussing particularly on tryptophan, following different surface modifications by carbon nanotubes (CNT), carbon black (CB) and copper nanoparticles. The modified electrodes were characterised by cyclic voltammetry, electrochemical impedance spectroscopy and scanning electron microscopy. Detection by square wave voltammetry was improved by further surface modification with copper nanoparticles, exhibiting efficient electrocatalytic activity towards amino acid oxidation with high sensitivity, stability and long shelf-life. The applicability of a low-cost, robust carbon black substrate using the synergetic electrocatalytic effect provided by copper nanoparticles for amino acid sensing is demonstrated.

Keywords: Screen printed electrodes, Carbon nanotubes, Carbon black, Copper nanoparticles, Amino acids

DOI: 10.1002/elan.201200499

1 Introduction

Amino acids, as essential building blocks of biological molecules, play key roles in many neurochemical response mechanisms, such as memory, appetite control and pain transmission [1,2]. Modern biochemical and pathological studies on cancer cells point to fluctuating nutrient levels between normal and cancerous cells. Many studies have proven that variations in the concentrations of essential amino acids in mammals such as tryptophan, aspargine, tyrosine, homocysteine etc. can act as biomarkers for cancer growth and in gene expression. The determination of amino acids is extremely important, as they are often added to food samples during their preparation in order to correct for possible dietary deficiencies [3–5]. One of the 20 essential amino acids for humans is tryptophan (Trp). It is a vital constituent of proteins, being a precursor of the neurotransmitter serotonin and indispensable in human nutrition for establishing a positive nitrogen balance.

During the past decade, numerous procedures involving high-performance liquid chromatography (HPLC) have been successfully developed and implemented for the determination of amino acids [6], but in recent years a detection methodology that does not require derivatisation is preferred, when available, for convenience and simplicity [7]. Furthermore, in some cases the quantitative detection of certain compounds is not necessary; only a qualitative detection is needed, as in the case of contamination, where the presence of certain contaminants by itself indicates the unacceptable quality of food. One of the possibilities for the rapid determination of amino acids is that of electrochemical methods. Since amino acids have at least two active functional groups (depending on pH): $-NH_2$ and –COOH, they have the ability to complex some transition metals (e.g. nicke1 [8] and copper [9])). One of the easiest metal ions to complex is copper as the Cu(II) ion.

Electrochemical methods have found many applications in the determination of electroactive amino acids. Tryptophan (Trp), tyrosine (Tyr) and cysteine (Cys) are examples of amino acids that, due to the inherent electroactivity of their thiol or aromatic groups, give an electrochemical response [10]. Various electrode materials such as carbon, platinum and gold are used [11], but, unfortunately, the voltammetric response is not satisfactory, because of slow heterogeneous electron transfer [12]. Therefore, it is necessary to employ physically and chemically modified electrodes in order to improve the ease of anodic oxidation of this kind of amino acids [13].

Carbonaceous nanomaterials have had immense impact in the material world, in various domains including electrocatalysis. Among them single-/multiwalled carbon nanotubes and fullerenes are attractive due to their excel-

lent physicochemical properties. Carbon nanotubes have unique properties [14], due to their high chemical stability, high mechanical stiffness, thermal conductivity, semiconductor behaviour, field emission, electrochemical actuation and electrochemical bond expansion [15–17]. As electrode materials, they can be used to enhance electron transfer between the electroactive species and the electrode [18–20], very useful for the development of bio- and chemical sensors. The incorporation of a catalyst or a redox mediator has increased the applicability of CNTs, usually multiwalled CNT (MWCNT); the integration of metallic nanoparticle, as catalysts, attracting much interest in the construction of electrochemical sensors because of their low ohmic contact resistance in composite structures [21,22]. Decoration with transition metal nanoparticles, including gold, platinum, palladium, copper, and silver [23–27] has been used to increase electrochemical activity.

Contrastingly, the above-mentioned bright prospects for the use of carbon nanotubes and fullerenes are overshadowed by the prohibitively high production costs and issues with purity. Ozawa and Osawa, [28], undertook an extensive comparative evaluation of the production costs of these carbonaceous nanomaterials and pointed out the huge production costs of nanotubes, especially single-walled CNTs. Moreover, alterations in the properties of these nanoproducts occur depending on source, synthetic strategy, manufacturers etc. which has been quantitatively studied in the case of electrochemical properties of MWCNTs by our group [29]. Hence, there is a need to explore cost-effective materials as electrode modifiers, especially for disposable-type sensors such as screen printed electrodes for bio- or environmental monitoring. In the present work, we have selected a suitable candidate viz. carbon black that has large scale production and extremely low production cost, almost 50 thousand fold less expensive than MWCNT, and excellent purity and homogeneity [28,30]. In addition, previous studies have proved the better biocompatibility of carbon black compared to nanotubes [31]. These micro/nanostructured materials, with a large number of defect sites, are frequently used as a catalyst support in fuel cells [32,33], because of their relative high stability in both acid and basic media, good electronic conductivity [34] and high specific surface area [35]. Only a few applications have been reported on the use of CB as electrode material for analyte detection in solution [30,36]. In addition to carbon black, copper nanoparticles, rather inexpensive compared to their noble metal counterparts, were also selected as electrode modifier owing to their active interaction with amino acids [9,37].

Screen printed electrodes (SPE) represent one of the most interesting and cost-effective alternatives in the design of electrochemical sensors for biomedical, environmental and industrial analyses [38,39]. The characterisation and the identification of edge plane site/defects role in carbon screen printed electrodes (SPE) [40,41], shows that the analytical performance can be improved by increasing the amount of such sites, making CNT and CB ideal for modifying SPE. In this study, SPEs were used as substrate for different modifications (CNT, CB, Cu), in order to evaluate and improve the determination of amino acids, focusing particularly on tryptophan at physiological pH. Further, the feasibility of composite electrodes using CB/Cu and CNT/Cu couples has been examined and a cost-effective sensing platform successfully developed using the synergistic electrocatalytic effect of carbon black and copper nanoparticles.

2 Experimental

2.1 Apparatus

The SPEs were a gift from the University of Rome "Tor Vergata" produced using a 245 DEK (Weymouth, England) screen-printing machine. The working and counter electrodes were printed with graphite-based ink (Elettrodag 421) from Acheson (Milan, Italy) and the pseudo-reference electrode with silver ink on a flexible polyester film substrate (Autostat HT5) obtained from Autotype Italia (Milan, Italy). Finally, an insulating ink was used to define the area of the working electrode surface. A curing period of 10 min at 70 °C was used. The diameter of the working electrode was 0.30 cm, corresponding to a geometric area of 0.070 cm^2.

The surface morphology of the SPEs and modified SPEs was examined using a scanning electron microscope (Jeol JSM-5310 (Jeol, Tokyo, Japan), equipped with an electronically controlled thermionic field emission gun. All images were captured at 20 kV.

All voltammetric experiments were carried out using a PalmSens portable electrochemical analyser (Palmsens BV, Houten, Netherlands) with PS-Lite software. CV experiments were carried out using a scan rate of 50 $mV\,s^{-1}$; and SWV parameters were: pulse frequency 10 Hz, amplitude 50 mV, and step potential 2 mV.

Electrochemical impedance spectroscopy was performed using the same three-electrode electrochemical system (SPE) and a 1250 Frequency Response Analyser, coupled to a Solartron 1286 Electrochemical Interface (Ametek, UK) controlled by ZPlot software. The sinusoidal voltage perturbation was 10 mV rms and the frequency range used was 65 kHz down to 0.1 Hz with 10 frequencies per decade, and an integration time of 60 s. Fitting of spectra was done with ZView software.

The pH measurements were done with a CRISON 2001 micro pH-meter (Crison, Spain). All experiments were performed at room temperature, 25 ± 1 °C.

2.2 Materials and Reagents

Multiwalled carbon nanotubes were obtained from Sigma (Germany) with >90 % purity, 110–170 nm diameter and 5–9 μm length.

Commercial Carbon Black, type N220, with a surface area of 120 $m^2\,g^{-1}$ was obtained from Cabot Corporation

(Ravenna, Italy). Nafion 5% solution in ethanol was from Aldrich (Germany), and acetonitrile from Merck, Germany.

Stock solutions in water of 10 mM amino acid were prepared using L-tryptophan, L(−)-tyrosine and L(−)-cysteine, all from Merck, Germany.

Acetate buffer and potassium chloride electrolyte solutions were prepared from reagents obtained from Riedel-de-Haën, Germany; Na_2SO_4 and $CuSO_4$ were purchased from Panreac, Spain.

Millipore Milli-Q nanopure water (resistivity >18 MΩ cm) was used for preparation of all solutions. Experiments were performed at room temperature, 25 ± 1 °C.

2.3 Electrode Pretreatment

The electrode surface was conditioned at +1.6 V for 120 s and at +1.8 V for 60 s, in 0.0025 mM acetate buffer solution (pH 4.6) plus 50 mM KCl (necessary because of the silver ink pseudo-reference) before voltammetric measurements. The application of high positive potentials in acidic media appears to increase the hydrophilic properties of the electrode surface via the introduction of oxygenated functionalities by oxidative cleaning [34].

2.4 Preparation of MWCNT-Modified SPEs

MWCNTs were purified and functionalised by stirring in 3 M nitric acid solution for 24 h. The solid product was collected on a filter paper and washed several times with nanopure water until the filtrate pH became nearly neutral. The functionalised MWCNTs were then dried in an oven at ≈80 °C for 24 h. Nitric acid causes significant destruction of carbon nanotubes and introduces –COOH groups at the ends of, or at the sidewall defects in, the nanotube structure [41,42]. The MWCNT-Nafion suspension was made by adding 0.5 mg MWCNT in 1 mL 0.1% Nafion solution (in ethanol) and then sonicating in an ultrasonic bath for 1 h. Chosen volumes (2–10 μL) of this suspension were dropped onto the SPE and left to dry for a minimum of 4 h.

2.5 Preparation of CB-Modified SPEs

The surface area and dimension of carbon black particles depend largely on the production method [6]. In this work, a commercial furnace-produced CB, N220, was employed. It was functionalised in a concentrated nitric acid solution during 24 h with stirring; the functionalised CB obtained was then dried in an oven at 80 °C for 24 h. In order to obtain a stable dispersion of CB with good reproducibility, the SPEs were modified with CB via "film" deposition, in which a CB dispersion was prepared in acetonitrile in order to achieve rapid solvent evaporation and a faster sensor production. Previously, in [43], it was reported that CB N330, after ultrasound irradiation at room temperature and atmospheric pressure under nitrogen for about 44 min, forms carbon nanosheets of a few nanometres thickness. Thus, sonication was limited to 30 min because, according to [43], this is probably sufficient to reduce the number of particles present in each aggregate and to enhance solubilisation without changing the structure of the CB, producing a stable, homogeneous, ink-like suspension.

Different concentrations of the CB dispersion in acetonitrile were tried in tandem with electrochemical studies. Similar results were obtained for different loadings of CB but, after data analysis, it was decided to work with a concentration of CB dispersion equal to 1 mg mL^{-1}. The amount of CB N220 on the electrode was also optimised by varying the concentration and volume of the CB dispersion placed onto the working electrode surface. As in the case of CNT, after modification the electrodes were dried in air.

2.6 Preparation of Copper-Modified Electrodes

Copper nanoclusters were electrochemically deposited on the modified CB/SPE and CNT/SPE electrodes at −1.0 V vs. Ag/AgCl in 0.1 M Na_2SO_4 + 2.0 mM $CuSO_4$ solution deoxygenated by high purity nitrogen for 10 min [27]. The modified electrodes prepared were CB/SPE, CNT/SPE, Cu/SPE, Cu/CB/SPE and Cu/CNT/SPE.

3 Results and Discussion

3.1 Optimisation of Modified Electrode Preparation

3.1.1 Choice of the Loading of CNT and CB

The choice of the amount of CNT and CB loading on the electrode surface for optimum sensor performance was assessed by monitoring the peak current as a function of Trp concentration by square wave voltammetry. Figure 1 shows that the oxidation response of Trp increases with the amount of CNT deposited on the electrode surface up to that corresponding to a CNT volume of 6 μL, above

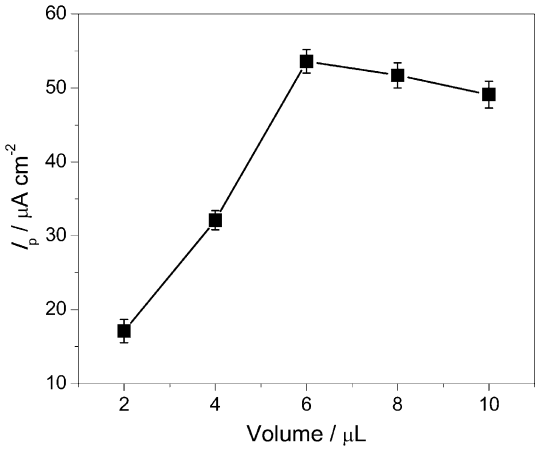

Fig. 1. Relation between the oxidation peak current of 100 μM Trp in 0.1 M KCl and the volume (amount) of CNTs placed on the SPE surface.

Table 1. Dependence of the Trp (100 μM) oxidation peak current on preconcentration potential on the Cu modified SPEs; preconcentration time 60 s.

Preconcentration potential (V)	Peak Current (I_p/μA)		
	Cu/SPE	Cu/CNT/SPE	Cu/CB/SPE
0.0	7.4 ± 0.6	27.1 ± 0.9	12.2 ± 0.6
−0.1	8.6 ± 0.7	32 ± 1.1	14.4 ± 0.9
−0.2	10.3 ± 0.7	32.1 ± 0.7	18 ± 1.2
−0.3	11.0 ± 0.6	29 ± 1.6	17 ± 1.1
−0.5	10.5 ± 0.8	25 ± 1.2	16.7 ± 0.9
−0.7	9.6 ± 0.5	23 ± 1.1	15 ± 1.0

which the peak current response decreased slightly. This may be due to an increase of the film thickness that hinders the movement of charge, decreasing the electrical conductivity [29].

Similar observations were made regarding the modification with carbon black. The optimum volume of CB was found to be 8 μL in separate additions of 2 μL, above which the Trp oxidation response decreases due to the blockage of electron transfer pathways.

3.1.2 Preconcentration Potential of Trp

The preconcentration potential and deposition time of Trp are also important factors to take into account, since the amperometric response of the modified screen printed electrodes is affected not only by the loading of CNT or CB but also by Cu nanoparticles deposited. The influence of the preconcentration potential on the response was investigated and the results are shown in Table 1. The response current of the modified sensors increases with more negative potential until −0.2 V, significant increases occurring in the presence of Cu nanoparticles until −0.3 V. However, for preconcentration at even more negative potentials (≤ −0.3 V) a decrease in the oxidation peak current of Trp is observed. In agreement with previous results [44–46], an increase in the current at 0.0 V was observed (data not shown) due to the oxidation of Cu_2O on the surface of the Cu nanoparticles to CuO in the presence of the amino acid, followed by formation of a complex between Cu (II) and Trp, according to:

$$Cu(II) + 2Trp^- \rightarrow Cu(Trp)^+ + Trp^- \rightarrow Cu(Trp)_2 \qquad (1)$$

From the values in Table 1, the maximum response for the different modifications occurs for a deposition potential of around −0.2 V, this potential being chosen for further work. At this potential there is a reversible equilibrium between $Cu^{II}O$ and $Cu^{I}O$, and the $Cu^{II}O/Cu^{I}O$ enriched surfaces are efficient for the stable and selective complexation of amino acids [46]. Hence, it can be concluded that surface adsorption of Cu(II) amino acid complexes results in effective preconcentration and this, along with the CuO mediated electrooxidation of tryptophan, leads to a cumulative signal enhancement.

When the preconcentration potential of −0.2 V was maintained for more than 60s, the tryptophan signal was found to decrease since the $Cu^{II}O/Cu^{I}O$ equilibrium is shifted towards Cu(I)O, resulting in shifting of the equilibria involving the copper-tryptophan complex in Equation 1 towards free Cu(II). This effect is greater at applied potentials more negative than −0.3 V, where there is an immediate decrease in the oxidation peak current, since in these conditions Cu(0) can also be formed, as observed in [44]. These facts indicate the crucial role of the Cu(II)O/Cu(I)O/Cu(0) reversible system for obtaining the optimum analytical signal for tryptophan.

3.1.3 Preconcentration Time of Trp

The oxidation peak current of 100 μM Trp at the modified electrodes increased with increase in preconcentration time until 60 s, above which it decreased slowly, see Figure 2. This may be due to the reversible Cu^{I}/Cu^{II} equilibrium at −0.2 V. In the presence of amino acids, the equilibrium is shifted to Cu(II) amino acid complexation up to a certain limit, beyond which the equilibrium is shifted in the opposite direction resulting in the formation of Cu(I) oxide and the amino acids are desorbed [44]. A nonconstant response was observed, as evidenced by the increase of the relative error.

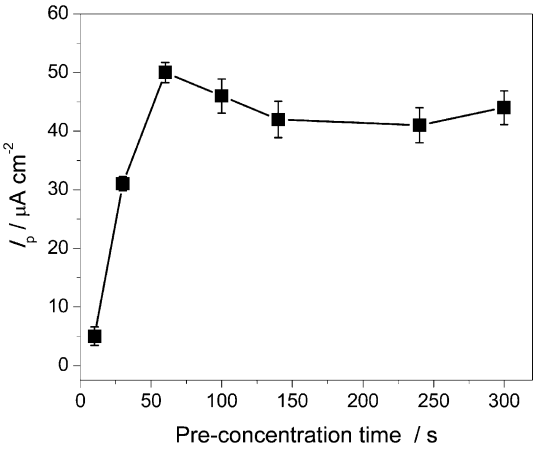

Fig. 2. Dependence of the 100 μM Trp oxidation peak current for 100 μM Trp in 0.1 M KCl on preconcentration time at the Cu-CNT modified electrode.

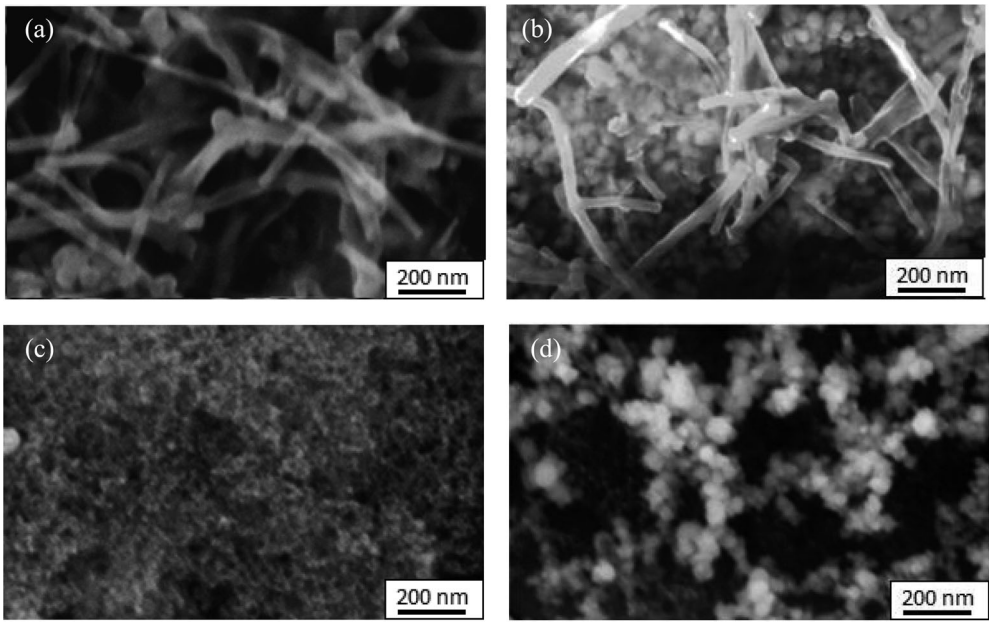

Fig. 3. Scanning electron micrographs of: (a) CNT/SPE, (b) Cu/CNT/SPE, (c) CB/SPE, (d) Cu/CB/SPE.

3.2 Characterisation of SPE Modified Electrodes

3.2.1 Morphological Characterisation of the SPE Modified Electrodes

Scanning electron microscopy (SEM) observations reveal that the nanosized copper particles are deposited and distributed over the surface of the SPE modified with functionalised CB and CNT, Figure 3. In the SEM images, the difference between the samples with and without deposited copper is easily seen; for both modifications the copper nanoparticles have similar diameters of ~40 nm and are aggregated in nanoclusters. It is also observed that in the case of CNT the amount of deposited copper is higher than for CB. This may be due to the large surface area provided by CNT modified electrodes compared to that of CB modified ones as evident from the CV studies discussed below. Also, the greater presence of Cu nanoparticles on the surface in the case of Cu/CB/SPE can be noticed from SEM micrographs. This predominance of copper nanoparticles on the CB surface points to the homogeneity and close packing of carbon black particles compared to CNT so that the interstitial voids are too small for penetration of copper nanoparticles to occur.

3.2.2 Cyclic Voltammetry

Cyclic voltammetry (CV) was used to characterise the SPE modifications by carbon nanotubes and carbon black. Cyclic voltammograms of 3.0 mM $Fe(CN)_6^{4-}$ in 0.1 M KCl at bare SPE, CB/SPE and CNT/SPE are shown in Figure 4. The electroactive surface area was calculated using the Randles–Sevčik equation:

$$I_p = 2.69 \times 10^5 \, AD^{1/2} n^{3/2} v^{1/2} C \quad (2)$$

where I_p is the oxidation peak current (in A), A is the electroactive area (in cm^2), D is the diffusion coefficient of the electroactive species (in $cm^2\ s^{-1}$), n is the number of electrons transferred, v is the potential scan rate (in $V\,s^{-1}$) and C is the concentration of the redox species in bulk solution (in $mol\,cm^{-3}$). The quasi-reversible one electron redox behaviour of hexacyanoferrate (II) ions was observed at the bare SPE with a peak separation of 100 mV at a scan rate of $50\ mV\,s^{-1}$. After being modified with the nanoparticles, the peak currents increased, while ΔE_p decreased compared to the bare SPE. The larger increase of electroactive area was for the CNT modification, resulting in an area of 0.17 cm^2, which is much larger than geometric area of 0.070 cm^2, whereas the modification with CB showed a smaller increase of 23 % (Figure 4).

The response after depositing Cu on the modified electrodes was also studied, the Cu/SPE modification showing an enhancement in current and a more reversible behaviour (Figure 4). An increase in the redox peak current was observed for both Cu/CB/SPE and Cu/CNT/SPE and, although the response continues to be higher for electrodes modified with CNT, the relative increase of response (in the presence of copper as compared to its absence) was higher for the SPE modified with CB, indicating that a different surface phenomenon is occurring. This anomalous behaviour of CB in the presence of copper nanoparticles can be explained on the basis of the reduction in surface area of CB after functionalisation, as reported by Carmo and co-workers [35]; they showed that the introduction of oxygenated functionalities in carbon black upon nitric acid functionalisation causes pore blockage. This pore blockage results in the preferential electrodepo-

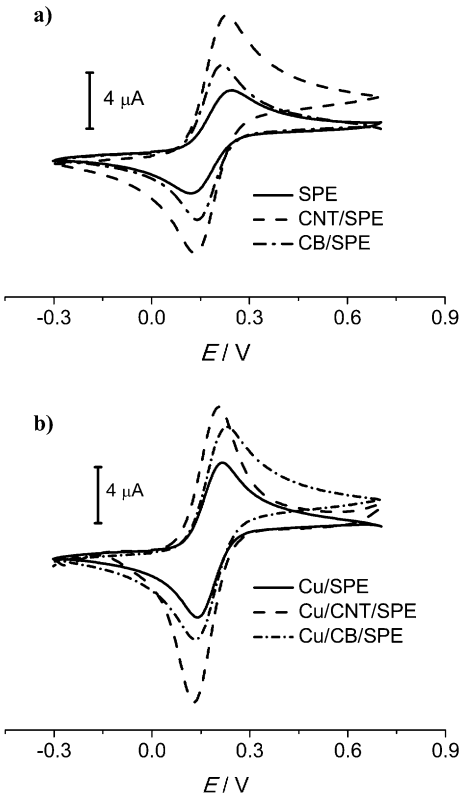

Fig. 4. Background subtracted cyclic voltammograms of 3 mM $K_4Fe(CN)_6$ in 0.1 M KCl at SPEs modified with (a) CNT and CB (b) copper-modified CNT and CB, at 50 mV s^{-1}.

sition of copper nanoparticles on the outer surface of CB, thereby enhancing the interaction with amino acids. Hence, a synergetic effect of the Cu/CB modified substrate can cause efficient enrichment of Cu(II)/amino acid complexes at the electrode surface and subsequent CuO-mediated electroxidation.

3.2.3 Electrochemical Impedance Spectroscopy

The unmodified electrodes and those modified with CB and CNT were characterized by EIS. Measurements were performed in 0.1 M KCl at 0.70 V. Since the data show a tendency for depressed semicircles, a constant phase element (*CPE*), rather than a simple capacitor, was employed to represent the charge separation in the interfacial region [43], according to the relation $CPE = -1/(Ci\omega)^{\alpha}$, where C is the capacitance (describing the charge separation at the double layer interface), ω is the angular frequency and α is the roughness factor (due to heterogeneity and nonuniformity of the surface). Different electrical equivalent circuits were tested to fit the spectra, by nonlinear least squares fitting, leading to use of the same electrical circuit for all spectra consisting of the cell resistance, R_{Ω}, in series with a parallel combination of a constant phase element, *CPE*, and a charge transfer resistance, R_{ct}, with an average error (χ^2) for the different modifications of $<3\times10^{-4}$. For bare SPEs, the R_{ct} was removed, due to the resistive behaviour of unmodified SPE.

Complex plane impedance spectra for all types of modified electrode are exhibited in Figure 5 together with the respective fitting, and values of the fitted parameters are given in Table 2. Observing the CPE values, the influence of the carbon modifications of SPE is easily seen, leading to an increase in the capacitance values by a factor of $\approx$6 for CB compared with bare SPE. In relation to the CNT modification, the increase of capacitance was by a factor of $\approx$28. These changes with respect to bare SPE can be attributed to the structure of the functionalised MWCNT and the longer time that is required for electrolyte ions to penetrate into the electrode material and form sufficient double layer. For the electrodes modified with copper nanoparticles, a decrease in the impedance values is observed (Figure 5) revealing a much lower electron transfer resistance on Cu-modified electrodes. The results are consistent with the CV results, and demonstrate that Cu-carbon modified electrodes may provide better electron conduction pathways due to a synergistic effect, improving the electrochemical properties of these modified electrodes.

3.3 Electrocatalytic Oxidation of Tryptophan at the Surface of Nanoparticle Modified SPEs

3.3.1 Square Wave Voltammetry

The electrochemical reduction and oxidation of amino acids are usually irreversible and occur at relatively high negative and positive potentials, respectively. In several reports, tryptophan showed well-defined oxidation peaks at +0.70 to +0.85 V [13,47]. SWV was used to investigate the electrochemical behaviour of Trp in 0.1 M KCl and in the potential range from 0.0 to +1.1 V only one oxidation peak was observed. Figure 6 shows that for a bare SPE, the oxidation potential of Trp occurs at +0.798 V. On the CNT/SPE, Trp oxidation occurs at +0.691 V, showing

Table 2. Equivalent circuit fitting parameters of impedance spectra for unmodified and modified SPE in 0.1 M KCl

Electrode	R_{Ω} (Ω cm^2)	R_{ct}(kΩ cm^2)	C (mF cm^{-2} s$^{\alpha\,-1}$)	α
SPE	4.0	–	0.22	0.76
Cu/SPE	3.6	36.4	0.51	0.80
CNT/SPE	3.9	4.32	6.2	0.86
Cu/CNT/SPE	4.2	2.99	8.4	0.85
CB/SPE	3.9	7.00	1.2	0.81
Cu/CB/SPE	4.0	3.43	1.2	0.85

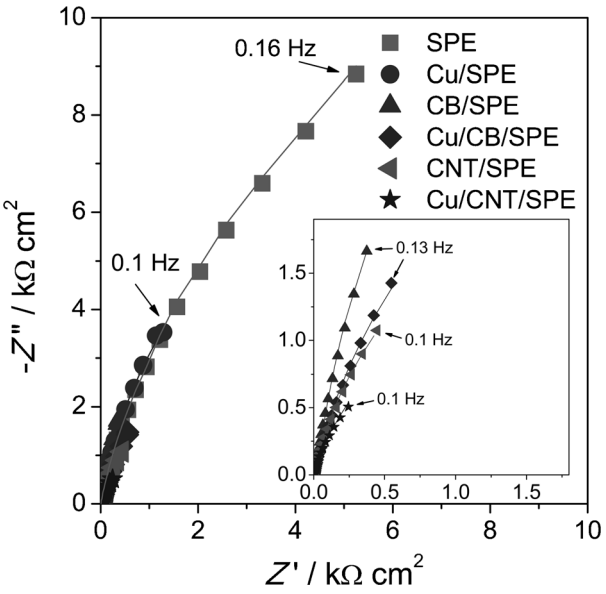

Fig. 5. Complex plane impedance spectra of modified SPE in 0.1 M KCl at 0.70 V vs. Ag pseudo-reference. The inset magnifies spectra for all modified electrodes except Cu/SPE. Lines show equivalent circuit fitting.

a negative shift in the peak potential of 0.11 V, indicating an electrocatalytic effect of the CNT. CB/SPE also enhances the electrochemical response towards Trp oxidation. Comparing CNT/SPE and CB/SPE, although the increase of the oxidation peak current and the decrease of the overpotential are greater for CNT, the CB particles do lead to electrocatalytic behaviour. The higher current for CNT/SPE was expected as its surface area was higher than that of CB/SPE.

For electrodes modified with Cu, even without any carbon nanoparticles the current response for Trp oxidation increases. Figure 6b shows that there is an approximately 1.5 fold increase in peak current that can be ascribed to a more efficient catalytic effect of the copper nanoparticles. Regarding CNT modification, Figure 6b demonstrates that the Cu/CNT hybrid can accelerate electron transfer and improve the electrochemical performance [48].

There are greater performance enhancements after depositing copper nanoparticles on functionalised CB. For non-functionalised CB, there is not much difference in the electrochemical response for Trp oxidation with or without copper (data not shown), suggesting that non-functionalised carbon black is inadequate for metal deposition. Functionalisation of the CB surface by nitric acid treatment introduces oxygenated functional groups, the chemical reactions changing the hydrophobic/hydrophilic character. Thus, the reactivity can be altered, the catalytic properties modified as well as polarities changed (zeta potential) [35,49–51]. This functionalisation enables the CB surface to anchor the metal nanoparticles, and thus improve the electrochemical properties of the modified electrode (see Figure 6b).Although in the overall analysis of the voltammograms obtained it is undeniable that the SPE modified with CNT show the best overall response for Trp oxidation, the CB/SPE leads to a greater negative shift in the oxidation peak potential in the presence of Cu nanoparticles, compared with that obtained for CNT/SPE with and without copper nanoparticles. Also and quite unexpectedly, the relative increase (with and without copper) in peak current is more in the case of Cu/CB than Cu/CNT. This interesting feature observed in the case of Cu/CB/SPE is due to the effective accumulation of copper nanoparticles on the exterior of the carbon black pore structure and thence better exposure of the nanoparticles to the amino acid moieties [35].

3.3.2 Electrochemical Impedance Spectroscopy

All spectra were fitted to the same equivalent circuit used previously for the characterisation of modified and unmodified carbon film electrodes (Section 3.2.3). The values of the parameters from the fitting circuits are presented in Table 3. From the first type of experiments (Figure 7) it is seen that the addition of Trp to the solution leads to a decrease of the charge transfer resistance (~55% for CB and ~84% for CNT modification) for all electrodes. The electrodes modified with copper presented a better electrochemical response in the presence of Trp, showing (Figure 7) decreases in R_{ct} of the order of 65% for Cu/CB/SPE and 90% for Cu/CNT/SPE, indicating that electron transfer is facilitated. As expected, the values of the capacitance for the modified electrodes also increase in the presence of Trp, due to an increase of the double layer charge accumulation; this is accompanied by an increase of the α exponent which means that at modified electrodes the surface becomes smoother and more uniform in the presence of the amino acid.

Table 3. Equivalent circuit fitting parameters of impedance spectra for unmodified and modified SPE in 0.1 M KCl + 0.5 mM Trp.

Electrode	R_Ω (Ω cm^2)	R_{ct} (kΩ cm^2)	C (mF cm^{-2} s$^{\alpha-1}$)	α
SPE	4.2	10.6	0.36	0.81
Cu/SPE	3.3	12.2	0.72	0.83
CNT/SPE	3.9	0.72	8.8	0.90
Cu/CNT/SPE	3.6	0.39	10.5	0.89
CB/SPE	3.5	3.1	1.6	0.88
Cu/CB/SPE	3.7	2.12	1.6	0.87

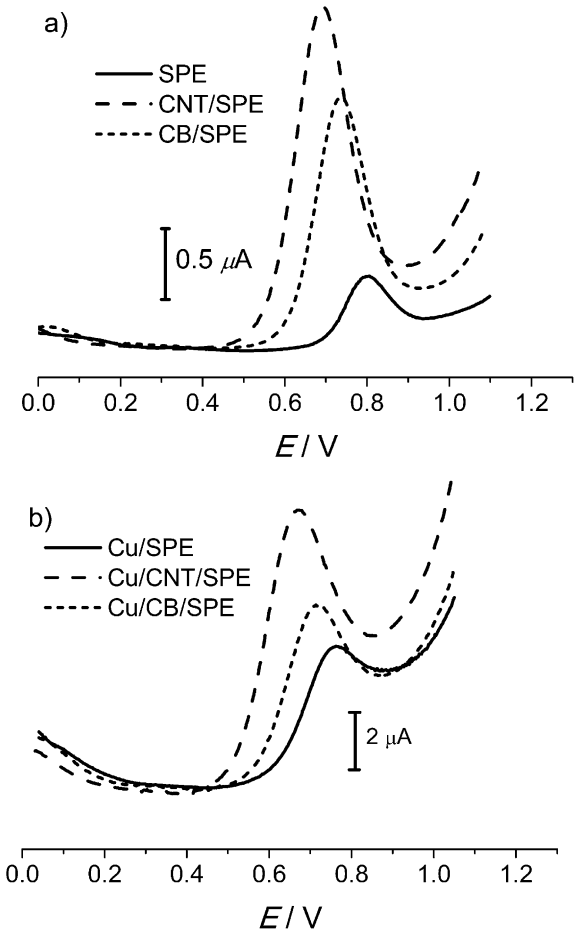

Fig. 6. SWV of 50 μM Trp in 0.1 M KCl for different modifications: a) SPE, CB/SPE and CNT/SPE; b) Cu/SPE, Cu/CB/SPE and Cu/CNT/SPE.

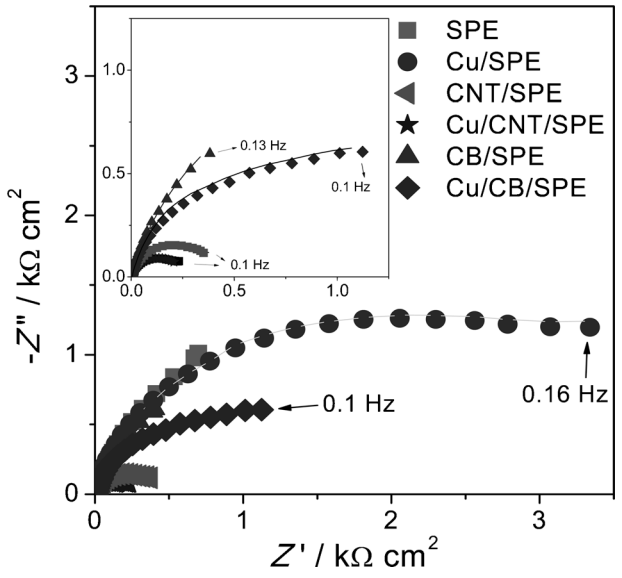

Fig. 7. Complex plane impedance spectra of modified SPE in 0.1 M KCl at 0.70 V vs. Ag pseudo-reference with 0.50 mM Trp. The inset magnifies spectra for all modified electrodes except Cu/SPE. Lines show equivalent circuit fitting.

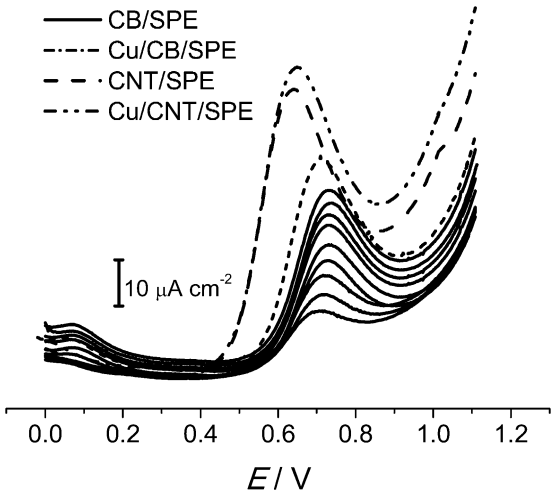

Fig. 8. SWV for different concentrations of Trp (—) from 10 to 150 μM in 0.1 M KCl for CB-modified SPE and after reaching 150 μM Trp for the other modified SPEs.

3.4 Analytical Parameters

The analytical performance of the CB/SPE is demonstrated from the SWV data in Figure 8, where different concentrations of Trp were injected into the operating cell. The current response peaks for increasing concentrations of Trp (10–150 μM) are clearly visible, with well-defined curves being observed after each addition. Further, it is also observed that in the presence of copper nanoparticles the CB/SPE show an increase in the current response as well as a decrease in the Trp oxidation potential. The lower oxidation potentials for nanoparticle modified SPEs represents an important advantage compared to bare electrodes; it reduce the response of interfering species during the analysis of natural samples where readily oxidisable interfering species may be present.

The response of the different modified electrodes to Trp oxidation increases linearly with concentration, as shown in the calibration plots (Figure 9) and in Table 4. As mentioned above, these plots show a higher sensitivity for the SPE modified with nanotubes (1.16 ± 0.07 μA μM^{-1} cm^{-2}) and a lower detection limit (1.41 μM) compared with CB/SPE, even more compared with the bare electrode. The detection limit was estimated from the signal-to-noise ratio ($S/N = 3$). It is important to stress that although the electrochemical response for the CNT/SPE changes slightly when modified with copper nanoparticles, for the CB/SPE the presence of the metal nanoparticles enhances the electrochemical properties of carbon black significantly due to synergetic electrocatalysis.

Other amino acids (cystine and tyrosine) which can be oxidised at the electrode surface [13,52], were selected to test the electrochemical response of the modified electrodes as well to carry out an interference study. The electrochemical response of the modified SPE to the oxidation of these amino acids was investigated and it was observed

Table 4. Analytical parameters for the determination of Trp, Tyr and Cys at SPE and modified SPE, in 0.1 M KCl, by SWV.

Electrode	Amino acid	*LOD* (μM)	Sensitivity ($\mu A\,\mu M^{-1}\,cm^{2}$)
SPE	Trp	24 ± 1.1	0.081 ± 0.002
	Tyr	80 ± 3.1	0.012 ± 0.002
	Cys	97 ± 5.1	0.007 ± 0.001
Cu/SPE	Trp	16.7 ± 0.9	0.12 ± 0.01
	Tyr	67 ± 1.2	0.013 ± 0.002
	Cys	101 ± 6.2	0.009 ± 0.001
CNT/SPE	Trp	1.41 ± 0.08	1.20 ± 0.07
	Tyr	34 ± 1.2	0.011 ± 0.002
	Cys	74 ± 2.2	0.051 ± 0.003
Cu/CNT/SPE	Trp	3.5 ± 0.3	1.11 ± 0.09
	Tyr	22.3 ± 0.9	0.091 ± 0.004
	Cys	82 ± 3.2	0.071 ± 0.003
CB/SPE	Trp	7.1 ± 0.6	0.41 ± 0.02
	Tyr	50 ± 1.4	0.051 ± 0.001
	Cys	88 ± 2.1	0.041 ± 0.001
Cu/CB/SPE	Trp	3.8 ± 0.21	0.05 ± 0.030
	Tyr	31.3 ± 0.9	0.009 ± 0.001
	Cys	82 ± 2.1	0.0021 ± 0.0002

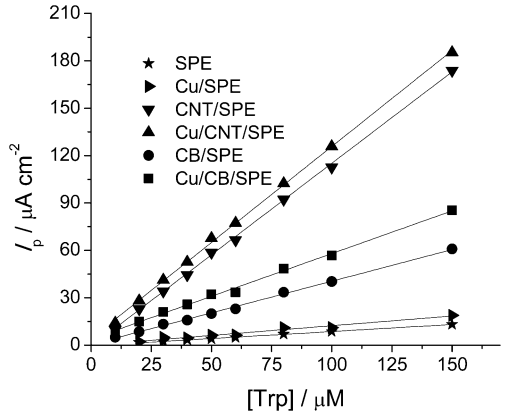

Fig. 9. Calibration curves calculated from SWV Trp oxidation peak current for different SPE modified electrodes.

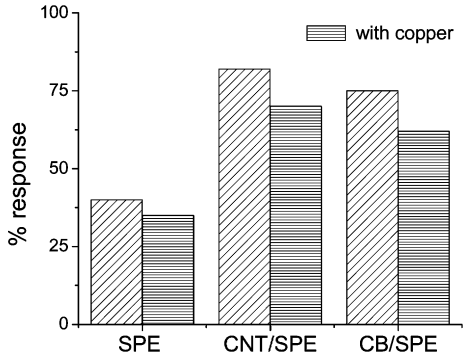

Fig. 10. Electrode response (%) after 8 consecutive CV scans (50 mV s^{-1}) for 100 μM Trp in 0.1 M KCl.

that the electrocatalytic effect for these amino acids does occur, but is small (smaller for CB) compared with the response for Trp. Table 4 shows the improvement in the *LODs* of the electrodes modified with CNT or CB, and the corresponding increase in sensitivity for the determination of Trp compared to Tyr and Cys. In relation to the determination of Trp in the presence of Cys and Tyr, the results show that for the CB/SPE and CNT/SPE there is no noticeable interference until concentrations are 10 fold greater that Trp. In addition, the CB and CNT electrodes modified with copper nanoparticles present a higher electrochemical response. Another notable feature was that copper modification lowers the *LOD* and sensitivity of CB/SPE electrodes without sacrificing the gain in selectivity. This is particularly advantageous for a low cost, robust and easily available electrode modifier for bio/environmental analyses.

Like most other organic molecules, Trp adsorbs easily onto electrode surfaces and can lead to electrode fouling after several measurements. Therefore 8 consecutive CV scans were made with 100 μM Trp, see Figure 10, showing an approximately 20% decrease for CB/SPE and CNT/SPE after the 8th scan. Although there is a decrease in the response, these results still demonstrate that the antifouling ability of nanostructured electrodes is much higher than the bare electrode, the unmodified SPE showing a decrease in the response of approximately 60%. Figure 10 also shows that the presence of copper nanoparticles leads to an increase of electrode fouling, that may occur due to the formation of Cu-Trp complexes at lower potentials [44].

Since oxidation of the amino acids at SPEs is prone to problems of surface passivation, the lifetime and storage of the different electrodes were also studied. The modified electrode stability was studied by measuring the voltammetric response after different storage periods. It was

observed that the SPE modified with carbon nanoparticles (CB and CNT) with and without Cu metal nanoparticles gave no apparent decrease in response after one week. The modified electrodes retained 95 and 88% of the initial response up to 15 and 30 days, respectively.

4 Conclusions

This paper demonstrates that the SPE are suitable for fast analysis and more importantly are a good substrate for nanoparticle modification. The experimental conditions, including the choice of the amount of CNT and CB, copper preconcentration time and potential were investigated. Furthermore, it was shown that CB, a material significantly cheaper than CNT, can be used in electrochemical sensor determinations. CB modified electrodes showed electrocatalytic properties and proved to be suitable for metal nanoparticle deposition, observed by the synergistic effect obtained with the copper nanoparticles that lead to an improvement in the electrochemical response on Trp determination. The excellent features of CB modified electrodes such as simple fabrication, low cost, high stability and biocompatibility ensures a promising future in clinical and food analysis. The commercial appeal of these materials can be further increased, by optimizing the production method of these electrodes, imprinting the Cu/CB particles in the SPE together with the carbon ink.

Acknowledgements

This work was supported by the *European Commission 7th Framework Programme Marie Curie Actions People IRSES* N°230815 NANOSENS, by *Fundação para a Ciência e a Tecnologia* (*FCT*), PTDC/QUI-QUI/116091/2009, POCH, POFC-QREN (co-financed by *FSE and European Community Fund FEDER/COMPETE*) and *CEMUC* (Research Unit 285), Coimbra, Portugal. RGC thanks *FCT* for a doctoral grant SFRH/BD/46496/2008 and KP for a postdoctoral grant SFRH/BPD/78939/2011.

References

[1] A. J. Meijer, P. F. Dubbelhuis, *Biochem. Biophys. Res. Commun.* **2004**, *313*, 397.
[2] D. Tome, *Br. J. Nutr.* **2004**, *92*, 27.
[3] H. D. Belitz, W. Grosch, R. Schieberle, *Food Chemistry*, 3rd ed., Springer, Berlin **2004**.
[4] M. I. Mohamed, C. Cordle, *Dev. Food Sci.* **2000**, *41*, 181.
[5] H. Masuda, A. Odani, T. Yamazaki, T. Yajima, O. Yamauchi, *Inorg. Chem.* **1993**, *32*, 1111.
[6] B. Deore, T. Nagaoka, *Anal. Sci.* **2001**, *17*, i1691.
[7] B. A. Deore, H. Shiigi, T. Nagaoka, *Talanta* **2002**, *58*, 1203.
[8] B. S. Hui, C. O. Huber, *Anal. Chim. Acta* **1992**, *134*, 211.
[9] J. N. Ye, R. P. Baldwin, *Anal. Chem.* **1994**, *66*, 2669.
[10] S. M. Macdonald, S. G Roscoe, *Electrochim. Acta* **1997**, *42*,1189.
[11] Y. D. Zhao, B. Zhang, Y. Liao, *Sens. Actuators B* **2003**, *92*, 279.
[12] W. Fang-Hui, Z. Guang-Chao, W. Xian-Wen, Y. Zhou-Sheng, *Microchim. Acta* **2004**, *144*, 243.
[13] Y. Liu, L. Xu, *Sensors* **2007**, *7*, 2446.
[14] S. Iijima, *Nature* **1991**, *354*, 56.
[15] L. M. Huang, J. Zia, S. O'Brian, *J. Mater. Chem.* **2007**, *17*, 3863.
[16] M. Pumera, S. Sanchez, I. Ichinose, J. Tang, *Sens. Actuators B* **2007**, *123*, 1195.
[17] W. R. Yang, P. Thordarson, J. Gooding, S. Ringer, F. Braet, *Nanotechnology* **2007**, *18*, 412001.
[18] Y. C. Tsai, S. C. Li, S. W. Liao, *Biosens. Bioelectron.* **2006**, *22*, 495.
[19] M. L. Pedano, G. A. Rivas, *Electrochem. Commun.* **2004**, *6*, 10.
[20] R. R. Moore, C. E. Banks, R. G. Compton, *Anal. Chem.* **2004**, *76*, 2677.
[21] S. Guo, S. Dong, *Trends Anal. Chem.* **2009**, *28*, 96.
[22] S. Guo, J. Li, W. Ren, D. Wen, S. Dong, E. Wang, *Chem. Mater.* **2009**, *21*, 2247.
[23] D. H. Marsh, G. A. Rance, R. J. Whitby, F. Giustiniano, A. N. Khlobystov, *J. Mater. Chem.* **2008**, *18*, 2249.
[24] X. G. Hu, T. Wang, L. Wang, S. J. Guo, S. J. Dong, *Langmuir* **2007**, *23*, 6352.
[25] V. A. Pedrosa, R. Epur, J. Benton, R. A. Overfelt, A. L. Simonian, *Sens. Actuators B* **2009**, *140*, 92.
[26] X. L. Ren, X. W. Meng, D. Chen, F. Q. Tang, J. Jiao, *Biosens. Bioelectron.* **2005**, *21*, 433.
[27] S. Wu, H. T. Zhao, H. X. Ju, C. G. Shi, J. W. Zhao, *Electrochem. Commun.* **2006**, *8*, 1197.
[28] M. Ozawa, E. Osawa, *Carbon Nanotechnology* (Ed: L. Dai), Elsevier, Dordrecht **2006** ch. 6.
[29] R. C. Carvalho, C. Gouveia-Caridade, C. M. A. Brett, *Anal. Bioanal. Chem.* **2010**, *398*, 1675.
[30] F. Arduini, F. Di Nardo, A. Amine, L. Micheli, G. Palleschi, D. Moscone, *Electroanalysis* **2012**, *24*, 743.
[31] *Safety of Nanoparticles. From Manufacturing to Medical Applications* (Ed: T. J. Webster), Springer, Heidelberg **2009**, ch. 8.
[32] A. R. Hopkins, N. S. Lewis, *Anal. Chem.* **2001**, *73*, 884.
[33] R. Alcantara, L. M. Jimenez-Mateos, P. Lavela, J. L. Tirado, *Electrochem. Commun.* **2001**, *3*, 639.
[34] M. E. Rice, Z. Galus, R. N. Adams, *J. Electroanal. Chem.* **1983**, *143*, 89.
[35] M. Carmo, M. Linardi, J. G. Poco, *Appl. Catalysis A: General* **2009**, *355*, 132.
[36] F. Arduini, C. Majorani, A. Amine, D. Moscone, G. Palleschi, *Electrochim. Acta* **2011**, *56*, 4209.
[37] C. W. Yang, J. M. Zen, Y. L. Kao, C. T. Hsu, T. C. Chung, C. C. Chang, C. C. Chou, *Anal. Biochem.* **2009**, *395*, 224.
[38] J. P. Hart, A. Crew, E. Crouch, K. C. Honeychurch, R. M. Pemberton, *Anal. Lett.* **2004**, *37*, 789.
[39] O. Domínguez Renedo, M. A. Alonso-Lomillo, M. J. Arcos Martínez, *Talanta* **2007**, *73*, 202.
[40] Q. Li, X. Zhang, G. Wu, S. Xu, C. Wu, *Ultrason. Sonochem.* **2007**, *14*, 225.
[41] E. Lahiff, C. Lynam, N. Gilmartin, R. O'Kennedy, D. Diamond, *Anal. Bioanal. Chem.* **2010**, *398*, 1575.
[42] L. Agüí, L. P. Yáñez-Sedeño, J. M. Pingarrón, *Anal. Chim. Acta* **2008**, *622*, 11.
[43] F. Arduini, A. Amine, C. Majorani, F. Di Giorgio, D. Felicis, F. Cataldo, D. Moscone, G. Palleschi, *Electrochem. Commun.* **2010**, *12*, 346.
[44] J. M. Zen, C. T. Hsu, A. S. Kumar, H. J. Lyuu, K. Y. Lin, *Analyst* **2004**, *129*, 841.
[45] R. P. Deo, N. S. Lawrence, J. Wang, *Analyst* **2004**, *129*, 1076.

[46] A. Sadkowski, *J. Electroanal Chem.* **2000**,*481*, 222.
[47] C. Li, Y. Ya, G. Zhan, *Colloid Surf. B, Biointerf.* **2010**, *76*, 340.
[48] Y. Guo, S. Guo, Y. Fang, S. Dong, *Electrochim. Acta* **2010**, *55*, 3927.
[49] T. Zhicheng, L. Qiuye, L. Gongxuan, *Carbon* **2006**, *45*, 41.
[50] Y. Liu, X. Qu, H. Guo, H. Chen, B. Liu, S. Dong, *Biosens. Bioelectron.* **2006**, *21*, 2195.
[51] H. Shioyama, K. Honjo, M. Kiuchi, Y. Yamada, A. Ueda, N. Kuriyama, T. Kobayashi, *J. Power Sources* **2006**, *161*, 836.
[52] M. Vasjari, A. Merkoçi, J. P. Hart, S. Alegret, *Microchim. Acta* **2005**, *150*, 233.

